Computation and field experiment validation of greenhouse energy load using building energy simulation model

Taehwan Ha[1], In-bok Lee[1,2], Kyeong-seok Kwon[1], Se-Woon Hong[3*]

(1. *College of Agriculture and Life Sciences, Seoul National University, 1 Gwanak-ro, Gwanak-gu, Seoul 151-921, Korea*;
2. *Research Institute of Agriculture and Life Sciences, 1 Gwanak-ro, Gwanak-gu, Seoul 151-921, Korea*;
3. *Institute for Agricultural and Fisheries Research (ILVO), Burg. Van Gansberghelaan 115, 9820 Merelbeke, Belgium*)

Abstract: Greenhouse Building Energy Simulation (BES) models were developed to estimate the energy load using TRNSYS (ver. 16, University of Wisconsin, USA), a commercial BES program. Validation was conducted based on data recorded during field experiments. The BES greenhouse modeling is reliable, as validation showed 5.2% and 5.5% compared with two field experiments, respectively. As the next step, the heating characteristics of the greenhouses were analyzed to predict the maximum and annual total heating loads based on the greenhouse types and target locations in the Republic of Korea using the validated greenhouse model. The BES-computed results indicated that the annual heating load was greatly affected by the local climate conditions of the target region. The annual heating load of greenhouses located in Chuncheon, the northernmost region, was 44.6% higher than greenhouses in Jeju, the southernmost area among the studied regions. The regression models for prediction of maximum heating load of Venlo type greenhouse and widespan type greenhouse were developed based on the BES computed results to easily predict maximum heating load at field and they explained nearly 95% and 80 % of the variance in the data set used, respectively, with the predictor variables. Then a BES model of geothermal energy system was additionally designed and incorporated into the BES greenhouse model. The feasibility of the geothermal energy system for greenhouse was estimated through economic analysis.

Keywords: Greenhouse, building energy simulation (BES), energy load, dynamic analysis, geothermal energy, heating load
DOI: 10.3965/j.ijabe.20150806.2037

Citation: Ha T, Lee I B, Kwon K S, Hong S W. Computation and field experiment validation of greenhouse energy load using Building Energy Simulation model. Int J Agric & Biol Eng, 2015; 8(6): 116－127.

1 Introduction

Greenhouses are essential in the farming industry for the stable production of high-quality crops year round, and it contributes positively to the rural economy. The total area of greenhouse greatly increased to 53 125 hm^2 in 2012[1]. Because of high heating cost rate and dependence of energy on overseas, reducing heating cost through efficient operations and management is a challenge for greenhouse farmers as well as agricultural industry. Optimizing the power of a heating system is also an important task in greenhouse management, which should be a priority for farm management and for achieving energy savings as well as savings on the initial cost of the system. For this reason, it has become increasingly important to precisely compute the heating load for the greenhouses before construction. Various renewable energy sources and energy saving technologies that can be adapted to greenhouses have been actively developed to reduce the heating cost of the greenhouse. Among the renewable energies, geothermal energy

Received date: 2015-06-26 **Accepted date:** 2015-11-30
Biographies: Taehwan Ha, PhD candidate, Research interests: aero-dynamics, building energy simulation, and computational fluid dynamics. Email: crown850@gmail.com; **In-bok Lee**, PhD, Professor, Research interests: aero-dynamics, building energy simulation, and computational fluid dynamics. Email: iblee@snu.ac.kr; **Kyeong-seok Kwon,** PhD candidate, Research interests: aero-dynamics, building energy simulation, and computational fluid dynamics. Email: kskwon0512@gmail.com.
***Corresponding author: Se-Woon Hong**, PhD, Scientific researcher, Institute for Agricultural and Fisheries Research (ILVO), Burg. Van Gansberghelaan 115, 9820 Merelbeke, Belgium, Email: hsewoon@gmail.com.

system is actively used in Korea, because it utilizes a relatively consistent underground temperature as an energy source throughout the year[2]. In Korea, the total area of greenhouses using geothermal heating systems increased from 38 hm^2 in 2011 to 116 hm^2 in 2013[3,4].

Static and dynamic energy analysis has been used to analyze the energy consumption because field experiment requires much more labor, time and cost. The static energy analysis method has an advantage that it has a simple procedure, easy to calculate compared with dynamic energy analysis method. However, the reliability and accuracy of these methods are relatively poor because they do not consider the effect of heat storage term and time-dependent changes in the climate conditions. In this sense, dynamic energy analysis method, such as building energy simulation (BES) can be a good alternative solution to more accurately compute the thermal energy flow under transient conditions.

BES was widely used to evaluate energy load of buildings by many researchers. Al-ajmi and Hanby[5] analyzed the internal air temperature of Kuwaiti domestic buildings according to wall type and window location using TRNSYS. Terziotti et al.[6] analyzed the heating load of large urban residential buildings equipped with a solar heating system. Furthermore, sensitivity analyses for the BES parameters were conducted to understand the energy performance[7,8]. Bhandari et al.[9] estimated the effect of the weather data quality because accurate weather data play an important role in analyzing building energy performance. Saelens et al.[10] developed a ray-tracing method and assessed cooling demand and required peak cooling power to describe solar transmittance of louver shading device. The energy performance for new construction designs was simulated to evaluate energy sustainability and cost effectiveness was compared to the conventional buildings[11]. Especially, Granadeiro et al.[12], Rahman et al.[13], Tzivanidis et al.[14], and Zogou and Stapountzis[15] estimated the energy consumption savings according to the building designs.

In the agricultural field, BES is also used to estimate energy loads. A heating energy for a commercial broiler house[16] and a peak and annual cooling (heating) loads of a glass-covered greenhouse were analyzed[17]. However, Hong et al. and Jang et al. did not conduct a validation experiment for their BES models. A deep-bed solar greenhouse was simulated to optimize the operation and design of a solar dryer[18]. The thermal behavior of an asymmetric greenhouse was estimated using a dynamic simulation[19]. The BES was also used to design and evaluate greenhouse-integrated systems, such as the seasonal solar soil heat storage system[20], and a proton exchange membrane fuel cell system[21].

TRNSYS is one of BES programs and it calculates the thermal energy flow based on the time-varying weather conditions, such as air temperature, humidity, wind direction and speed, and solar radiation. Because of its modular structure, a complex system to be simulated can be broken down into several components, and it gives flexibility and possibility of new user-created modules. In this study, TRNSYS was applied to investigate the time-varying heating load of greenhouse according to typical greenhouse types and six climatic conditions of domestic regions in Korea. The accuracy of the BES greenhouse model was initially examined using field experimental data. Even though plants influence the energy balance in the greenhouse, the amount of sensible and latent heat exchanges are not easy to assess because it varies according to plant species, growth stages and micro-environmental conditions. Therefore, in this study, the maximum heating load (MHL) and the annual heating load (AHL) of an empty greenhouse which did not raise any potential crops were estimated. Moreover, a BES geothermal system model was also designed and then it was integrated into the BES greenhouse model to analyze heating cost savings.

2 Materials and methods

2.1 BES

BES using TRNSYS was divided into energy rate control (ERC) and temperature level control (TLC) according to the heating or cooling system. ERC calculates energy load using calculated internal air temperature and designed internal air temperature based on energy flow. And TLC calculates internal air temperature considering operation of heating or cooling

system. In this Study, ERC is used to assess the heating load of greenhouse and TLC is used to simulate geothermal energy system.

The building module calculates energy flow, such as radiation, convection, radiant heat, and heat storage. The total quantities of thermal energy gain or loss ($\dot{Q}$) can be calculated by considering total heat gain or loss at surface ($\dot{Q}_{surf}$), heat gain or loss by ventilation ($\dot{Q}_{vent}$), internal convective heat gain or loss ($\dot{Q}_{gain}$), heat gain or loss from infiltration ($\dot{Q}_{\inf}$), heat gain or loss due to connective air flow from adjacent zone ($\dot{Q}_{cplg}$) and removed latent energy ($\dot{Q}_{lat}$). The TRNSYS estimates the internal air temperature and the energy loads of target building. The internal air temperature is calculated based on the operating of heating or cooling system, the thermal conductivity of wall, the radiation, and the energy loads are calculated based on the difference between the computed internal air temperature and set air temperature at every time-step.

$$\dot{Q}_i = \dot{Q}_{surf} + \dot{Q}_{vent} + \dot{Q}_{gain} + \dot{Q}_{inf} + \dot{Q}_{cplg} + \dot{Q}_{lat} \quad (1)$$

$$\dot{Q}_{surf} = A_s \cdot (q_{c,s} + q_{r,s}) \quad (2)$$

$$\dot{Q}_{vent} = \rho \cdot C_p \cdot N_{vent} \cdot V \cdot (T_{out} - T_{in}) \quad (3)$$

$$\dot{Q}_{inf} = \rho \cdot C_p \cdot N_{inf} \cdot V \cdot (T_{out} - T_{in}) \quad (4)$$

$$\dot{Q}_{cplg} = \rho \cdot C_p \cdot N_{cplg} \cdot V \cdot (T_{zone,i} - T_{in}) \quad (5)$$

$$\dot{Q}_{lat} = h_v[m_{inf}(\omega_a - \omega_{req}) + m_{vent}(\omega_{vent} - \omega_{req}) + W_g + m_{cplg}(\omega_{zone,i} - \omega_{req}) - M_{eff}\frac{d\omega}{dt}] \quad (6)$$

$$q_{c,s} = h_{conv}(T_s - T_{in}) \quad (7)$$

$$q_{r,s} = \sigma \cdot \varepsilon_s (T_s^4 - T_{in}^4) \quad (8)$$

where, A_s is inside area of surface, m^2; C_p is thermal capacity of air, kJ/kg·°C; ρ is air density, kg/m^3; $N_{vent,\,inf}$ is air rate of ventilation and infiltration, h^{-1}; N_{cplg} is air rate due to connective air flow from zone i infiltration, h^{-1}; $T_{in,\,out}$ is internal air temperature and external air temperature, °C; $T_{zone,\,i}$ is internal air temperature of zone i, °C; T_s is temperature of surface, °C; V is internal volume of greenhouse, m^3; h_v is heat of vaporization, kJ/kg; h_{conv} is convective heat transfer coefficient, kJ/h·m^2·°C; ω_a is ambient humidity ratio; ω_{req} is set-point for humidification or dehumidification; ω_{vent} is humidity ratio of ventilation air; $\omega_{zone,i}$ is humidity ratio of zone i; W_g is internal moisture gain; M_{eff} is effective moisture capacitance of zone; σ is Stephan-Boltzmann constant, kJ/h·m^2·$°C^4$; ε_s is long wave emissivity.

2.2 Target facilities

2.2.1 Experimental greenhouse for the BES validation

The validation of the BES greenhouse model was conducted at a 6-span Venlo-type greenhouse located in Gimje City, Korea (latitude: 35.51°N, longitude: 126.55°E). The greenhouse without any crops was selected to validate the estimations of the internal air temperature and energy load of the BES greenhouse model. Figure 1 showed the experimental multi-span Venlo-type greenhouse, which was composed of six spans that were 19.2 m in width, 52 m in length, 5.76 m in ridge height and 4.8 m in eaves height while the internal floor area was 998.4 m^2.

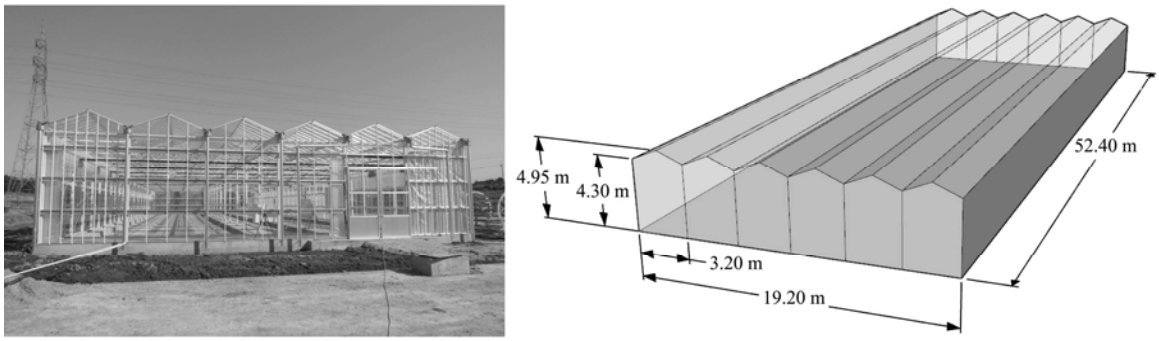

Figure 1 Photo and schematic diagram of the experimental greenhouse in Gimje city, Republic of Korea used for the BES validation

2.2.2 BES greenhouse models

BES greenhouse models were designed using commercial glass-covered greenhouses to estimate the heating load of the greenhouses according to local weather conditions, greenhouse type, and the number of spans. The dimensions of the greenhouses were

designed based on the Korean greenhouse standard for Venlo type and Widespan type[22]. The structural specifications of greenhouses are presented in Table 1, and schematic diagrams of each greenhouse are presented in Figure 2.

Table 1 Structural specifications of the greenhouses[22]

Type of greenhouse	Venlo			Widespan		
	2-span	6-span	8-span	2-span	5-span	8-span
Model name (Korea standard of greenhouse structure)	RDA · 97-B-I			RDA · 97-A-I		
Ridge height/m	4.95			6.5		
Eaves height/m	4.3			4.3		
Number of spans	2	6	8	2	5	8
Width of span/m	3.2	3.2	3.2	9.0	9.0	9.0
Width of greenhouse/m	6.4	19.2	25.6	18.0	45.0	72.0
Length of greenhouse/m	45.0	45.0	45.0	45.0	45.0	45.0
Floor area of greenhouse/m^2	288.0	864.0	1152.0	810.0	2025.0	3240.0
Surface area of greenhouse/m^2	757.1	1497.2	1867.2	1483.0	3127.1	4771.1
Volume of greenhouse/m^3	1332.0	3996.0	5328.0	4374.0	10 935.0	17 496.0
Surface area/Floor area	2.63	1.73	1.62	1.83	1.54	1.47
Volume/Floor area/m	4.63	4.63	4.63	5.4	5.4	5.4

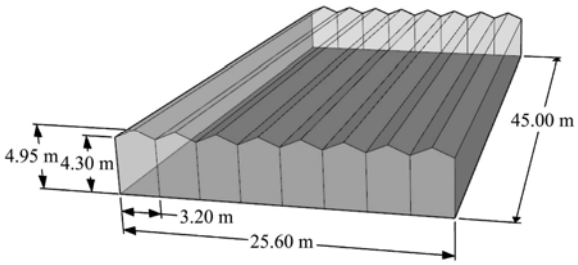

a. 8-span Venlo type greenhouse

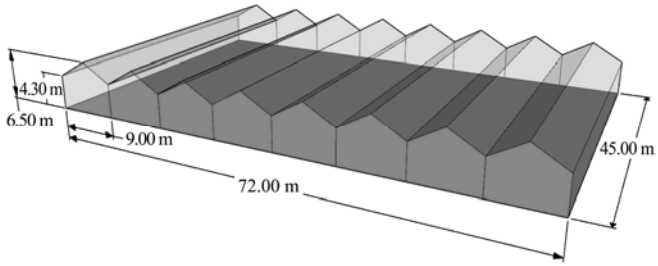

b. 8-span Widespan type greenhouse

Figure 2 Schematic diagrams of the experimental multi-span greenhouses used in the study

2.2.3 Geothermal energy system

A geothermal energy system is primarily composed of a ground heat exchanger, a Ground Source Heat Pump (GSHP), a heat storage tank, and a heat supply system. The GSHP and heat supply system used in this study were a water–water type heat pump (GTHP-C110AA, Top-sol Co., Korea) and fan coil unit (FC-P80, Kiturami homesys Co., Korea) commonly used in Korea. Also a closed loop ground heat exchanger that uses ground heat as the heat source was generally used to prevent contamination of the ground water in Korea. The schematic diagram of geothermal energy system is shown in Figure 3 and the specifications of geothermal energy system are shown in Table 2.

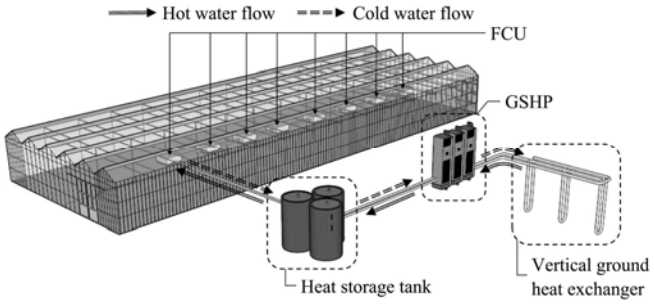

Figure 3 Schematic diagram of the geothermal energy system including GSHP, vertical ground heat exchanger, heat storage, FCU

Table 2 Specifications of the GSHP (GTHP-C110AA, Top-sol Co., Korea), ground heat exchanger, heat storage tank, and fan coil unit (FC-P80, Kiturami homesys Co., Korea)

Content		Specification
GSHP	Model	GTHP-C110AA
	Heating capacity/W	114 995
	Active power of electricity/W	30 995
	Flow rate/$L \cdot s^{-1}$	7.33
	COP	3.71
	Cost/$\$ \cdot EA^{-1}$	17 272.8
Closed-loop vertical ground heat exchanger	Depth of borehole/m	150
	Radius of borehole/m	0.075
	Thermal conductivity of soil/$W \cdot m^{-1} \cdot K^{-1}$	3.6
	Cost/$\$ \cdot m^{-1}$	19.1
Heat storage tank	Diameter/m	6.2
	Height/m	8.0
	Capacity/m^3	240
Fan coil unit	Model	FC-P80
	Heating capacity/W	19 771
	Flow rate/$L \cdot min^{-1}$	28
	Cost/$\$ \cdot EA^{-1}$	271.0

2.3 Experimental procedure

The BES validation model was designed using material properties and dimensions of the experimental greenhouse. The BES model was validated by comparing the BES computed and measured internal air temperatures. Then the validated modules and methodologies were adopted to design six BES greenhouse models to estimate the heating load according to the greenhouse types and climate conditions. Additionally, a BES module for the geothermal energy system was designed and combined. The heating costs of greenhouse when geothermal energy system was

adopted were compared to the heating cost when conventional oil boiler was used. Figure 4 presents the experimental procedure.

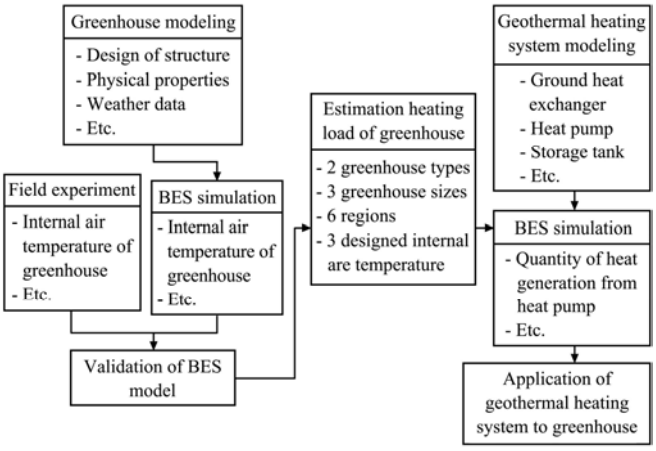

Figure 4 Flow chart of the experimental procedure

2.3.1 Validation of the BES greenhouse model

In the experimental greenhouse, HOBO sensors (H08-032-08, Onset computer corp., USA), and a portable weather station (Watchdog 2900ET, Spectrum Technologies INC., USA) were used to measure air temperature, humidity, solar radiation and wind speed and direction. The first experiment was conducted from February 27, 2012 to February 29, 2012 and the second experiment was conducted from May 5, 2012 to May 7, 2012. The portable weather station was installed in an open area near the greenhouse to measure the external air temperature, humidity, solar radiation, wind direction, and wind speed at a 1 min interval. The internal air temperature of the experimental greenhouse was measured at the 13 points at a height of 1.5 m using HOBO sensors during the 1st field experiment and at 18 points at heights of 0.2 m, 2.0 m, and 4.0 m during 2nd field experiment (Figure 5). The measured outdoor environment conditions were used as inputs of the BES simulation, and the measured indoor thermal data were used to examine the accuracy of the BES greenhouse model.

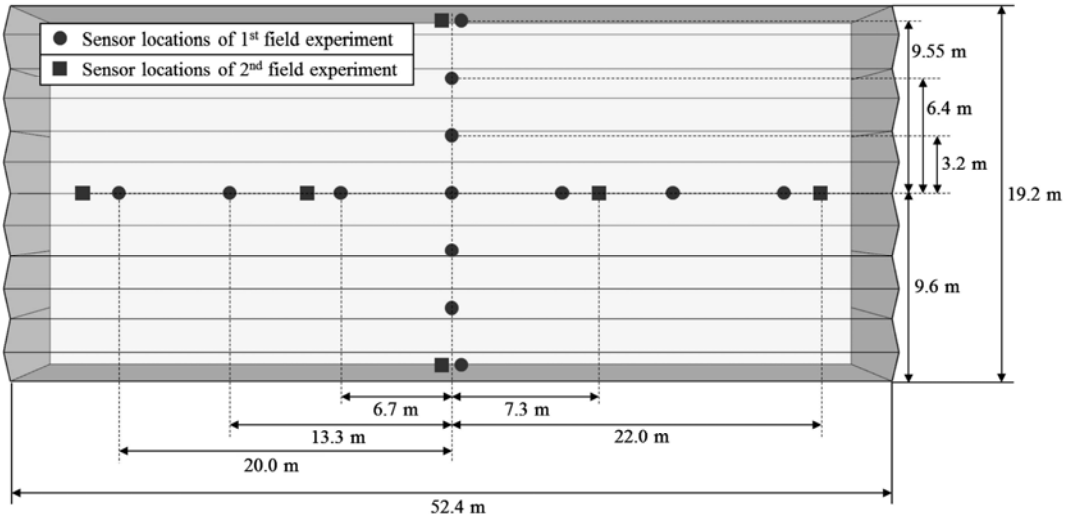

Figure 5 HOBO sensor locations in the greenhouse of two field experiments; (HOBO sensors were located at a height of 1.5 m in the 1st field experiment and the sensors were located at heights of 0.2 m, 2.0 m, and 4.0 m in the 2nd field experiment

Because the greenhouse walls were glass, the amount of radiant solar energy flowing into the greenhouse was affected by properties of the glass and ratio of the frames, which affect the heating and cooling loads. Therefore, the glass properties and frame ratio of the target greenhouse were utilized to design surface of BES greenhouse model. Solar transmittance, solar reflectance, visible transmittance, visible reflectance, thermal infrared transmittance, infrared emittance, conductivity (W/m·K), and u-factor (W/m^2·K) of 5 mm glass generally used to greenhouse in Korea were 0.816, 0.071, 0.894, 0.08, 0, 0.837, 1.0, and 5.834, respectively, and the frame ratio was 10%[23].

TRNSYS drew a temperature in a zone based on the assumption that internal air of a zone was perfectly mixed. Because of this, BES computed heating load could be different according to zone division method. Therefore, various types of spatial division models, such as a single layer model, a 4 horizontal layers model, and a 6 vertical layers model, were designed as shown in Figure 6, and

then analyzed to determine which division method is appropriate to greenhouse modeling. The properties of greenhouse frame and floor are presented in Table 3.

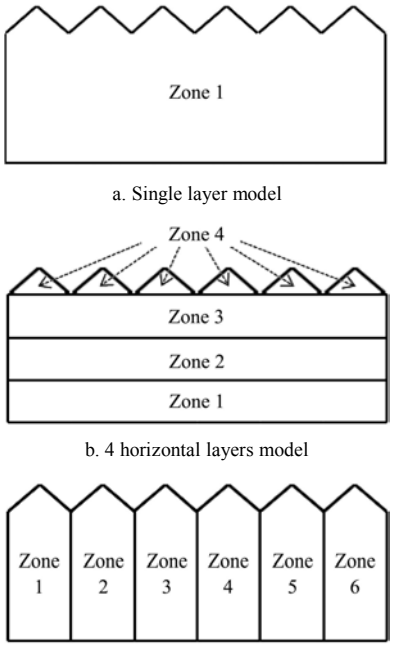

a. Single layer model

b. 4 horizontal layers model

c. 6 vertical layers model

Figure 6 Design of the BES greenhouse models by zone divisions

Table 3 Physical properties of the greenhouse frame and floor used in the BES simulation[23]

	Frame	Floor		
Materials	Stainless steel	Concrete	PE film	Gravel
Density/kg·m^{-3}	7800	2240	0.96	1800
Specific heat/kJ·kg^{-1}·K^{-1}	0.51	0.92	2.3	1.0
Thermal conductivity/kJ·h^{-1}·m^{-1}·K^{-1}	56.0	6.23	0.88	7.2
Thickness/m	0.05	0.3	0.001	0.2

2.3.2 Comparison of the heating load based on greenhouse type and climatic conditions

The main factors considered to estimate the MHL and AHL of greenhouses were as follows: 1) type of greenhouse (Venlo type and Widespan type), 2) number of spans with 3 sub-factors, 3) regions where the greenhouses were constructed [Chuncheon (central and southern inland mountain climate type), Suwon (central west coast climate type), Cheongju (central flatland climate type with excess rainfall), Daegu (basin climate type), Jeonju (southern flatland type with excess rainfall climate type) and Jeju (mild climate type)], and 4) designed internal air temperatures. The latitude and longitude of each region are presented in Figure 7.

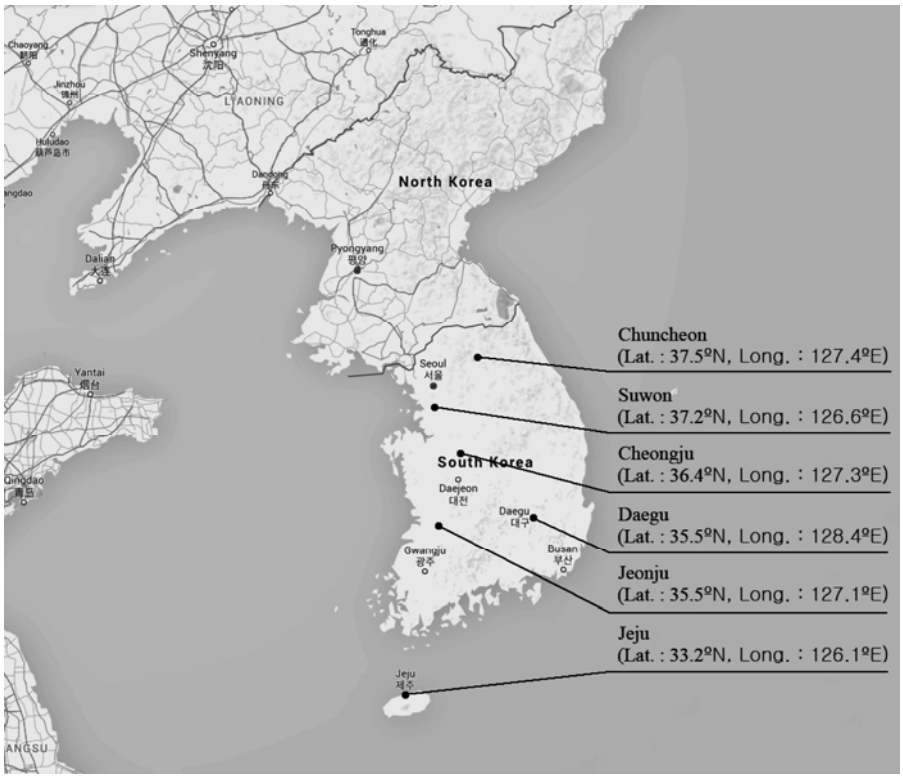

Figure 7 Latitude and longitude of the six regions selected for the study

The climate data for radiation, temperature, humidity, and underground soil temperature for each area in 2012 were obtained from the Korea Meteorological Administration (KMA) as design conditions for the simulation. A total of 8784 h of data from January 1 to December 31, 2012 were converted to a new format that can be applied to TRNSYS, and the heating load of the greenhouses was estimated by TRNSYS. The simulated

annual total heating load was analyzed using the annual sum of Heating Degree Hours (HDH; Equation (9))[24] and the annual sum of Heating Degree Temperature (HDT; Equation (10)).

$$HDH = \sum_{j=1}^{8784} (1) \text{ when } T_i(j) \le T_{set} \quad (9)$$

$$HDT = \sum_{j=1}^{8784} \{T_{set} - T_i(j)\} \text{ when } T_i(j) \le T_{set} \quad (10)$$

The designed internal air temperature was determined based on the optimum growth temperature of crops. High-temperature plants include melon, watermelon, and cucumber; medium-temperature plants include tomato, chrysanthemum, and rose; and low-temperature plants include strawberry, lettuce, and celery[25]. Because minimum air temperature of winter season in South Korea is sometimes below −20°C, Korea rural development administration suggested the optimum temperatures of the high-temperature plants, medium-temperature plants, and low-temperature plants during the nighttime as 12°C, 8°C and 5°C, respectively, to prevent frost damage and to save heating cost, while the optimum temperatures during daytime were 25°C, 23°C, and 12°C, respectively[25].

2.3.3 Geothermal energy system modeling and application

A closed-loop vertical ground heat exchanger was generally used for greenhouses in Korea, and the length of the ground heat exchanger was designed to be 11-16 m per 1 kW of GSHP capacity[26]. The capacity of the heat storage tank was designed to cover daily total heating load[27], and the capacities of the GSHP and fan coil unit were designed based on the MHL of greenhouse.

The operation of the GSHP depended on the water temperature of the heat storage tank. When the water temperature of the heat storage tank was lower than 40°C, the GSHP and the circulation pump were operated until the temperature of the heat storage tank reached the setting temperature (50°C). When the air temperature of the greenhouse was lower than the designed internal air temperature, the fan coil units were until the air temperature of greenhouse reached the designed internal air temperature.

We designed the BES geothermal energy system module of greenhouses in Chuncheon region to fully cover heating load of the greenhouses, and we compared heating costs of the greenhouses when the conventional heating system was replaced by the geothermal energy system. The heating costs of greenhouse with the geothermal energy system and greenhouse with the conventional oil boiler (DKE-600 & DKE-1500, Kiturami boiler Co., Korea) were calculated to estimate the heating cost saving and the payback period of the geothermal energy heating system compared to the conventional heating system, which used an oil boiler. The specifications of the conventional oil boiler are shown Table 4.

Table 4 Specifications of the conventional oil boiler (DKE-600 & DKE-1500, Kiturami boiler Co., Korea)

Content		Specification	
Conventional oil boiler	Model	DKE-600	DKE-1500
	Heating capacity/kW	450	1120
	Oil usage/L·h^{-1}	50.2	125.5
	Cost/$	11364	16728

3 Results and discussion

3.1 Validation of the BES greenhouse model

The first field experiment, which was conducted during the winter season, resulted in an average external air temperature of 1.3°C, and the average internal air temperature of the greenhouse was 7.6°C higher than the external air temperature. The external and internal maximum temperatures were observed at 14:00 on February 29, which were 15.2°C and 33.2°C, respectively, and the solar radiation was 2620 kJ/m^2·h. The second field experiment was conducted during the spring season. The average external air temperature was 17.8°C, and the average internal temperature of the greenhouse was 31.0°C. Over the three days, the internal air temperature of the greenhouse at 14:00 were 47.7°C, 53.4°C and 50.2°C, respectively, and the external air temperature were 21.8°C, 26.1°C, and 25.4°C, respectively.

As the first validation step, the BES computed resulted from three zone division methods were compared to the experimental data (Figure 8). The 6 vertical layers model was shown to have the most similar trend with the experimental data. During the first experimental period, the maximum difference between the BES computed results and measured results were 5.8°C, 8.0°C, and 3.3°C for single, 4 horizontal layers,

and 6 vertical layers models, respectively, with an average difference were 2.4°C, 2.5°C, and 1.1°C, respectively. Results of the second experimental period showed the maximum difference of 4.5°C, 3.6°C, and 4.4°C, respectively, and the average difference of 2.1°C, 2.6°C, and 1.1°C, respectively. For the 4 horizontal layers model, the highest internal air temperature values were found at the bottom section (zone 1) because the heat storage is located near the ground. While the air temperature of zone 1 was greatly increased, the air temperature of the other zones was not sufficiently affected by the heat storage. The internal air temperature of the 6 vertical layers model showed almost uniform across the sections because the effect of heat storage near the ground was effectively conveyed to entire volume of each zone.

Table 5 presents the BES calculated MHLs and the measured results during two field experiments. The measured MHL during first field experiment was calculated to be 23.9 GJ/h, and the BES calculated MHLs of the single, 4 horizontal layers, and 6 vertical layers models were 25.8 GJ/h, 26.2 GJ/h, and 25.2 GJ/h, respectively. In the second field experiment, the MHL for the target greenhouse was obtained as 35.6 GJ/h, while the BES computed results showed the MHLs of 32.5 GJ/h, 31.6 GJ/h and 33.6 GJ/h for the single, 4 horizontal layers, and 6 vertical layers models, respectively. In the first experiment, the largest relative error of 9.6% and the smallest relative error of 5.2% were shown at the 4 horizontal layers model and the 6 vertical layers model, respectively. Similarly, the largest error of 11.3% and the smallest error of 5.5% in the 2nd field experiment were shown at the 4 horizontal layers model and the 6 vertical layers model, respectively. Therefore, it could be concluded that the "6 vertical layers model" predicted heating load more accurately than the others and the BES computed internal air temperature was well agree with the experimental data.

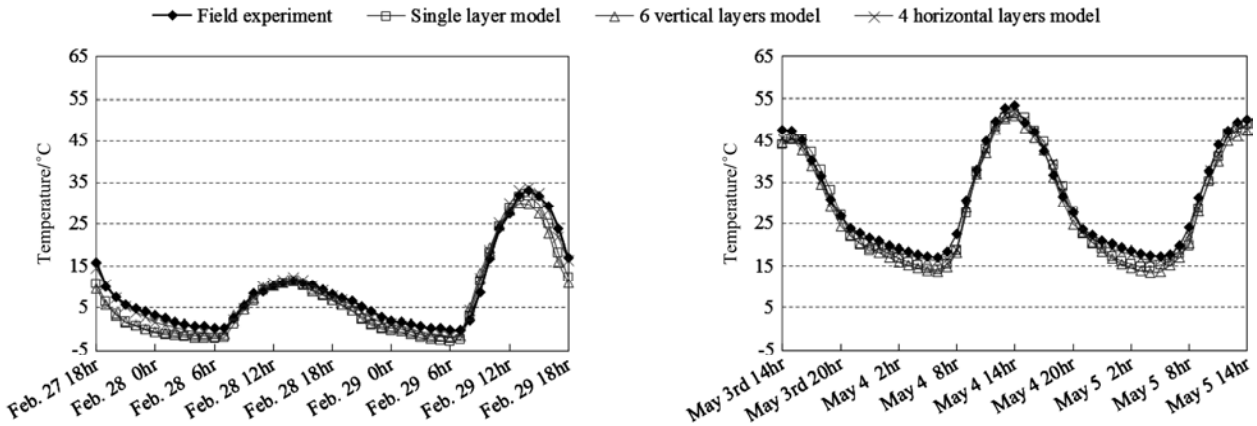

a. 1st field experiment b. 2nd field experiment

Figure 8 Comparison of internal air temperatures using measured data from the field experiment and computed data from the simulations

Table 5 Comparison of data measured from the field experiment and data computed from the BES simulation model for the first and second field experiments

			Measured	Single layer model	4 horizontal layers model	6 vertical layers model
1st Field Exp.	Difference of temperature with field experiment/°C	Maximum		5.8	8.0	3.3
		Average		2.4	2.5	1.1
	Heating load	MHL/GJ·h^{-1}	23.9	25.8	26.2	25.2
		Error/%		8.0	9.6	5.2
2nd Field Exp.	Difference of temperature with field experiment/°C	Maximum		4.5	3.6	4.4
		Average		2.1	2.6	1.1
	Heating load	MHL/GJ·h^{-1}	35.6	32.5	31.6	33.6
		Error/%		8.7	11.3	5.5

3.2 Estimation of maximum and annual total heating load of greenhouses

The MHL and the AHL of all cases are summarized in Tables 6 and 7. The Widespan type greenhouse had higher MHLs than the Venlo type greenhouse, and the MHLs of the 8-span greenhouses were higher than the

loads of the 2-span and 5-span greenhouses.

Table 6 Maximum heating load (MJ/h) of the greenhouses based on the greenhouse type, regions, and designed internal air temperature

		Venlo			Widespan		
Region	Designed internal air temperature	2-span	6-span	8-span	2-span	5-span	8-span
Cheongju	HT*	484	982	1278	926	2086	3347
	MT**	462	949	1235	885	2005	3216
	LT***	314	624	810	597	1328	2130
Chuncheon	HT	565	1118	1452	1067	2372	3803
	MT	544	1085	1409	1027	2290	3672
	LT	395	757	981	738	1612	2582
Daegu	HT	450	900	1170	849	1897	3042
	MT	428	865	1125	808	1814	2909
	LT	279	532	690	517	1125	1802
Jeju	HT	339	706	920	648	1476	2370
	MT	317	607	874	606	1391	2233
	LT	168	339	441	314	703	1128
Jeonju	HT	463	926	1205	875	1959	3141
	MT	441	892	1161	834	1877	3010
	LT	293	567	736	546	1200	1922
Suwon	HT	495	988	1284	936	2089	3351
	MT	473	954	1241	895	2008	3220
	LT	325	626	812	606	1328	2128

Note: * Optimum growth temperature for High-temperature plants: 25℃ in the daytime and 12℃ in the nighttime.

** Optimum growth temperature for Medium-temperature plants: 23℃ in the daytime and 8℃ in the nighttime.

*** Optimum growth temperature for Low-temperature plants: 12℃ in the daytime and 5℃ in the nighttime.

Table 7 Annual total heating load (GJ) of the greenhouses based on the greenhouse type, regions, and designed internal air temperature

		Venlo			Widespan		
Region	Designed internal air temperature	2-span	6-span	8-span	2-span	5-span	8-span
Cheongju	HT	720	1196	1541	1315	2654	4260
	MT	558	924	1190	1018	2049	3287
	LT	237	365	468	420	808	1293
Chuncheon	HT	819	1361	1752	1499	3023	4850
	MT	648	1071	1377	1184	2377	3812
	LT	310	482	618	552	1067	1708
Daegu	HT	548	882	1134	993	1961	3148
	MT	404	649	834	731	1439	2309
	LT	143	207	265	247	457	732
Jeju	HT	473	807	1044	866	1775	2854
	MT	340	596	772	626	1301	2093
	LT	77	120	155	136	264	425
Jeonju	HT	657	1091	1405	1200	2418	3881
	MT	498	826	1063	909	1827	2932
	LT	197	296	379	344	653	1045
Suwon	HT	719	1188	1529	1313	2638	4234
	MT	556	913	1174	1013	2027	3252
	LT	241	368	471	425	813	1300

In case of 8-span Widespan type greenhouse with HT, the highest MHL was 3803 MJ/h when the greenhouse was located in Chuncheon, which was 60.5% higher than the MHL of Jeju. A comparison between the regions showed that the MHL was related to the minimum external air temperature and the latitude. Among the target regions, Chuncheon was located in highest latitude and showed the lowest external air temperature during simulation periods, hence, the highest MHL was shown in Chuncheon.

Additionally, the AHLs showed the same tendency with the MHLs. The highest and lowest values of AHL were obtained from the 8-span Widespan type greenhouse situated in Chuncheon and the 2-span Venlo type greenhouse located in Jeju, respectively. When the HDT was high (HDT of Chuncheon was 87 837℃, and it was higher than the values from the other locations), the AHL was also high (the AHL of Chuncheon was higher than the other locations). Similar to the MHL, the highest AHL (4850 GJ) was shown when the greenhouse was located in Chuncheon, and it was 69.9% higher than the AHL of Jeju.

In the case of Chuncheon, the maximum heating load was 1452 MJ/h at 8:00 on February 2nd, when the external air temperature was −22.6℃, this was the lowest external air temperature of the day and the solar radiation was zero.

3.2.1 Comparison of heating loads according to the number of spans

In the case that the designed internal air temperatures were set for high-temperature plants, the MHLs of Venlo type greenhouse increased 101.5% and 162.0% as the number of span was increased from 2 to 6 and 8, respectively. The MHLs of Widespan type greenhouse also increased by 124.3% and 259.7% for 6 and 8 spans, respectively. When the designed internal air temperatures were set for medium-temperature plants and low-temperature plants, the MHLs also increased based on changing the number of spans. The AHLs showed a similar increasing tendency as the increasing rate of the MHLs of greenhouses. The average increasing rates of AHL of Venlo type greenhouse were 61.4% and 107.5% when the number of spans increased from 2 to 6 and

8-span, respectively. Additionally, the increasing rates of Widespan type greenhouse were 97.9% and 217.4%, when the number of spans was increased from 2 to 5 and 8-span, respectively

When the number of spans increased from 2 to 6 and 8, surface area increased by 97.8% and 146.6% for Venlo type greenhouses, respectively. Similarly, when the number of spans increased from 2 to 5 and 8, surface area increased 110.9% and 221.7% for Widespan type greenhouses, respectively. It was found that the increase of the MHL and AHL were highly related to surface area of the greenhouse because the larger greenhouse surface had larger heat losses.

3.2.2 Comparison of the heating loads according to region

The differences in the MHL between regions occurred due to the differences in the latitude and the lowest external air temperature of each region. Among the six regions, the highest MHL occurred in Chuncheon, the northernmost region, where the minimum external air temperature of −22.6°C was shown. Comparing with MHL of Venlo type greenhouse in Chuncheon, the MHLs for the Cheongju, Daegu, Jeju, Jeonju, and Suwon showed 14.9%, 23.3%, 44.4%, 20.3% and 13.9% lower values, respectively, and the MHLs for the Widespan type greenhouse from Cheongju, Daegu, Jeju, Jeonju, and Suwon showed 14.5%, 23.7%, 44.9%, 20.5% and 14.1% lower values, respectively. The lowest MHL occurred in Jeju, the southernmost location.

Among the six regions, the highest AHL occurred in Chuncheon, and it is related with the highest HDTs and the highest HDHs presented in Table 8. The AHL was also dependent on the latitude of regions, and showed a similar tendency as the MHL. Hence, the highest AHL was estimated for the greenhouse located in Chuncheon and the lowest AHL was obtained for the greenhouse located in Jeju (54.0% lower than that in Chuncheon).

Table 8 Annual accumulated heating degree hours (h) and annual accumulated heating degree temperature (°C) for the six regions

	Cheongju	Chuncheon	Daegu	Jeju	Jeonju	Suwon
HDH (rank)	5522 (3)	5928 (1)	5305 (6)	5371 (5)	5439 (4)	5634 (2)
HDT (rank)	74489 (3)	87837 (1)	64087 (5)	49532 (6)	69645 (4)	77520 (2)

3.3 Application of geothermal energy systems

The geothermal energy system model consisted of modules for a geothermal heat exchanger, a ground source heat pump, a heat storage tank, a fan coil unit and circulation pumps, and connections between the modules. The modular model is presented in Figure 9. The capacities of the geothermal energy system for the 8-span Venlo type greenhouse and 8-span Widespan type greenhouse were designed based on the estimated MHL of the greenhouses. There were 4 heat pumps for the 8-span Venlo type greenhouse and 10 for the 8-span Widespan type greenhouse, and the number of fan coil units for the greenhouses were 21 and 54, respectively, to cover the MHLs of greenhouses. The total lengths of the closed-loop vertical ground heat exchanger were 6464 m and 16 912 m, respectively; therefore, the number of boreholes were 44 and 113 holes with 150 m, respectively.

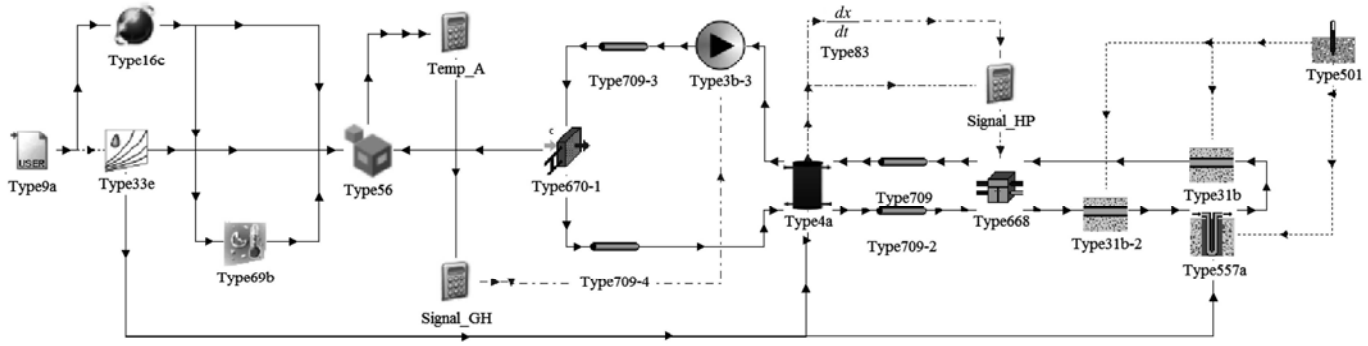

Figure 9 Schematic diagram of the geothermal energy system modeling using TRNSYS

An integrated simulation of the geothermal energy system and greenhouse models was conducted using the weather data from Chuncheon in 2012. The internal and external air temperatures of 8-span Venlo type greenhouse during January 30 to February 5, 2012 are shown in Figure 10. The heat pumps for the 8-span

Venlo type and Widespan type greenhouses were operated for 975 h and 1574 h, respectively, and the fan coil units for the 8-span Venlo type and Widespan type greenhouses were operated for 1764 h and 2303 h, respectively. The initial costs of the geothermal energy system for the 8-span Venlo type and 8-span Widespan type greenhouses were \$286 689 and \$717 129, respectively. Therefore, the annual heating costs of the 8-span Venlo type and Widespan type greenhouses with the geothermal energy system were calculated as approximately \$4350 and \$17 386, respectively, based on the electricity cost of Korea at 2012 (\$33.9 /MW·h). Meanwhile, when the conventional diesel boiler was used, the usages of diesel were approximately 56 000 L and 152 000 L, respectively, corresponding to heating costs of \$51 000 and \$139 000, respectively. The cost saving for the 8-span Venlo type and Widespan type greenhouses were approximately \$47 000 and \$122 000, respectively. The payback periods of the geothermal energy system of the 8-span Venlo type and Widespan type greenhouses were calculated 5.8 years and 5.7 years, respectively.

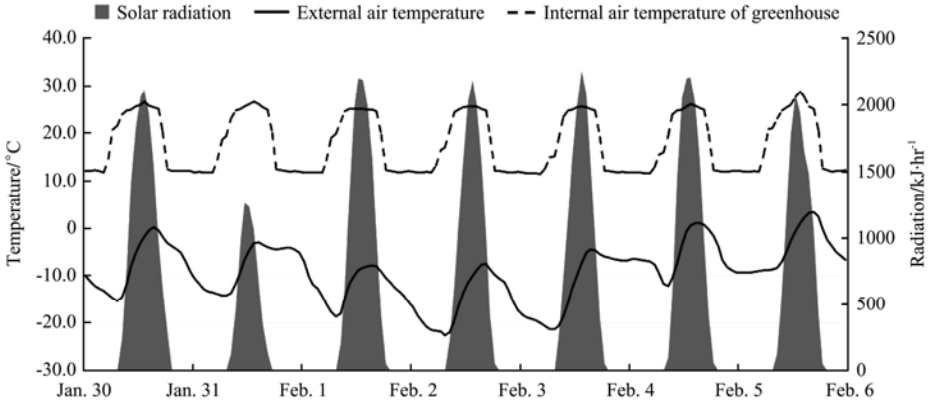

Figure 10 Internal and external air temperatures of the 8-span Venlo-type greenhouse with the geothermal energy system during Jan. 30 to Feb. 5, 2012 (the MHL was observed at 8:00 on Feb. 2, 2012)

4 Conclusions

The aim of this research was to study the heating load of greenhouse according to the type of greenhouse, region, and designed internal air temperature, and to integrate the geothermal energy system module into the BES greenhouse model. The conclusions are made as follow:

(1) The BES greenhouse model is validated by comparing the BES computed results to the measured results from the field experiments with about 5% error according to the spatial division method.

(2) The computed heating load from six different regions demonstrates that the heating load was higher in Chencheon (high latitude) than in Jeju (low latitude) and it is strongly related to both of the latitude and the external air temperature.

(3) The vertical type geothermal energy system installed in the multi-span glass covered greenhouse has the economic feasibility based on economic analysis.

Furthermore, we designed and validated a BES greenhouse model without crops because there is still a lack of information and knowledge to simulate crop phenomena in the BES. For future studies, heat transfer processes of crops will be integrated into the BES model to improve reality of BES greenhouse models.

Acknowledgements

This work was carried out with the support of the "Cooperative Research Program for Agriculture Science & Technology Development (Project No. PJ009412)" Rural Development Administration, Republic of Korea.

[References]

[1] Ministry of Agriculture, Food and Rural Affairs (MAFRA). Major statistics data of agriculture, food and rural affairs. 2014; 11-1543000-000128-10. (in Korean)

[2] Hanova J, Dowlatabadi H. Strategic GHG reduction through the use of ground source heat pump technology. Environmental Research Letters, 2007; 2(4): doi: 10.1088/1748-9326/2/4/044001.

[3] Ministry of Agriculture, Food and Rural Affairs (MAFRA). 2011 greenhouse status for vegetables and vegetable production records. 2011; 11-1541000-000273-10. (in Korean)

[4] Ministry of Agriculture, Food and Rural Affairs (MAFRA). 2013 greenhouse status for vegetables and vegetable production records, 2013; 11-1543000-000051-10. (in Korean)

[5] Al-ajmi F F, Hanby V I. Simulation of energy consumption for Kuwaiti domestic buildings. Energy and Buildings, 2008; 40(6): 1101–1109.

[6] Terziotti L T, Sweet M L, McLeskey Jr J T. Modeling seasonal solar thermal energy storage in a large urban residential building using TRNSYS 16. Energy and Buildings, 2012; 45: 28–31.

[7] Magnier L, Haghighat F. Multiobjective optimization of building design using TRNSYS simulations, genetic algorithm, and Artificial Neural Network. Building and Environment, 2010; 45: 739–746.

[8] Rodríguez G C, Andrés A C, Muñoz F D, López J M C, Zhang Y. Uncertainties and sensitivity analysis in building energy simulation using macroparameters. Energy and Buildings, 2013; 67: 79–87.

[9] Bhandari M, Shrestha S, New J. Evaluation of weather datasets for building energy simulation. Energy and Buildings. 2012; 49: 109–118.

[10] Saelens D, Parys W, Roofthooft J, de la Torre A T. Assessment of approaches for modeling louver shading devices in building energy simulation programs. Energy and Buildings, 2013; 60: 286–297.

[11] Lehmann B, Güttinger H, Dorer V, van Velsen S, Thiemann A, Frank Th. Eawag Forum Chriesbach—Simulation and measurement of energy performance and comfort in a sustainable office building. Energy and Buildings. 2010; 42: pp. 1958-1967.

[12] Granadeiro V, Duarte J P, Correia J R, Leal V M. Building envelope shape design in early stages of the design process: Integrating architectural design systems and energy simulation. Automation in Construction, 2013; 32: 196–209.

[13] Rahman M M, Rasul M G, Khan M M K. Energy conservation measures in an institutional building in sub-tropical climate in Australia. Applied Energy, 2010; 87(10): 2994–3004.

[14] Tzivanidis C, Antonopoulos K A, Gioti F. Numerical simulation of cooling energy consumption in connection with thermostat operation mode and comfort requirements for the Athens buildings. Applied Energy, 2011; 88(8): 2871–2884.

[15] Zogou O, Stapountzis H. Energy analysis of an improved concept of integrated PV panels in an office building in central Greece. Applied Energy, 2011; 88(3): 853–866.

[16] Hong S W, Lee I B, Hong H K, Seo I H, Hwang H S, Bitog J P, Yoo J I, Kwon K S, Ha T, Kim K S. Analysis of heating load of a naturally ventilated broiler house using BES simulation. Journal of the Korean Society of Agricultural Engineers, 2008; 50(1): 39–47. (in Korean with English abstract)

[17] Jang J C, Kang E C, Lee E J. Peak cooling and heating load and energy simulation study for a special greenhouse facility. Journal of the Korean Solar Energy Society, 2009; 29(1): 72–76. (in Korean with English abstract)

[18] Akghbashlo M, Müller J, Mobli H, Madadlou A, Rafiee S. Modeling and simulation of deep-bed solar greenhouse drying of chamomile flowers. Drying Technology, 2014; 33: 684–695.

[19] Alvarez-Sánchez E, Leyva-Retureta G, Portilla-Flores E, López-Velázquez A. Evaluation of thermal behavior for an asymmetric greenhouse by means of dynamic simulations. Dyna, 2014; 81(188): 152–159.

[20] Zhang L, Xu P, Mao J C, Tang X. Design and application of a seasonal solar soil heat storage system applied in greenhouse heating. Applied Mechanics and Materials, 2014; 672: 21–25.

[21] Vadiee A, Yaghoubi M, Sardella M, Farjam P. Energy analysis of fuel cell system for commercial greenhouse application–A feasibility study. Energy Conversion and Management, 2015; 89: 925–932.

[22] Ministry of Land, Transport and Maritime Affairs (MLTMA). The standard design of Korea glass greenhouses. 1997. (in Korean)

[23] Bok L S, Analysis and Validation of Dynamic Heat Energy for Greenhouse with Geothermal System using Field Data. MS thesis, Seoul: Seoul National University in Korea, 2012.8, 94p. (in Korea with English abstract)

[24] Flynn C, Sirén K. Influence of location and design on the performance of a solar district heating system equipped with borehole seasonal storage. Renewable Energy, 2015; 81: 377–388.

[25] Rural Development Administration (RDA). Weekly information for farming, 2011; 3.6-3.12. Suwon: National Institute of Agricultural Engineering of RDA. Republic of Korea, 2011. (in Korean)

[26] Doo L B. A study on optimum entering water temperature in vertical closed ground loop heat pump system. MS thesis, Seoul: Hanyang University in Korea, 2009.8; 93p. (in Korean with English abstract)

[27] Park Y, Kim K. A study on the horizontal ground source heat pump greenhouse heating system with thermal storage tank. Journal of Energy Engineering, 2006; 15(3): 194–201.